POLITECNICO DI TORINO
Repository ISTITUZIONALE

A resilience-aware methodology to support data center optimal allocation considering the transmission grid's hosting capacity

Original
A resilience-aware methodology to support data center optimal allocation considering the transmission grid's hosting capacity / Jr., G.M., Rozenblit Tiferes, R., Nascimento Ribeiro, T., Mazza, A., Pons, E.. - In: APPLIED ENERGY. - ISSN 0306-2619. - ELETTRONICO. - 423:(2026). [10.1016/j.apenergy.2026.128351]

Availability:
This version is available at: 11583/3013090 since: 2026-07-14T07:38:20Z

Publisher:
Elsevier Ltd

Published
DOI:10.1016/j.apenergy.2026.128351

Terms of use:

This article is made available under terms and conditions as specified in the corresponding bibliographic description in the repository

Publisher copyright

(Article begins on next page)

02 November 2026

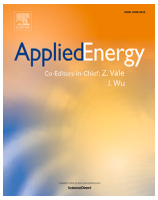
Applied Energy 423 (2026) 128351



Contents lists available at ScienceDirect

Applied Energy

journal homepage: www.elsevier.com/locate/apen



A resilience-aware methodology to support data center optimal allocation considering the transmission grid's hosting capacity☆

Giovanni Manassero Jr.[a], Rodrigo Rozenblit Tiferes[a,*], Thamiris Nascimento Ribeiro[a], Andrea Mazza[b], Enrico Pons[b]

[a] Departamento de Engenharia de Energia e Automação Elétricas, Escola Politécnica da Universidade de São Paulo, São Paulo, 05508-010, SP, Brazil
[b] Dipartimento Energia (DENERG) "Galileo Ferraris", Politecnico di Torino, Turin, 10129, Italy

HIGHLIGHTS

- Transmission-level analysis for integrating utility-scale data centers.
- Hosting capacity and region selection for optimal data center integration.
- Framework applicable across existing and planned transmission infrastructure.
- Resilience assessment under multiple contingency scenarios.

ARTICLE INFO

Keywords:
Data centers
Optimal allocation
Transmission grid
Hosting capacity
Resilience

ABSTRACT

The growing demand for digital services has driven the deployment of increasingly large data centers, with individual facilities expected to reach gigawatt-scale power requirements in the near future. However, integrating such large loads into existing transmission systems requires careful planning to ensure efficient and timely grid connections while minimizing environmental impacts. In this context, this article introduces a methodology to support the optimal allocation of new data centers within an existing transmission grid. The proposed approach relies on Particle Swarm Optimization and explicitly accounts for the grid's hosting capacity while identifying allocations that remain technically feasible under a predefined set of contingency scenarios. By jointly addressing capacity limits and operational resilience, it enables data center placements that operate within the transmission infrastructure's limits and preserve system security under adverse conditions. A case study based on a real transmission system with high-capacity data centers already in operation is presented, and the results indicate that the methodology can provide practical decision support for both transmission system planners and data center developers.

1. Introduction

1.1. Contextualization

The world is undergoing digital transformation. Data-driven applications and resources, such as artificial intelligence (AI), cloud computing, and big data analytics, are becoming increasingly prevalent across industries and in daily life. This rapid evolution and widespread adoption of digital platforms, however, have led to a significant increase in the number of data centers. As a result, the energy consumption of these facilities has grown substantially [1]. According to the International Energy Agency (IEA) report on energy and AI (April 2025) [2], data centers currently consume approximately 415 TWh annually, and by 2030, their consumption is projected to reach 945 TWh.

Today, several data centers operate at capacities on the order of hundreds of MW, sometimes even approaching the GW mark. However, to reduce their overall energy consumption and carbon footprint, many incorporate sustainable practices, such as job scheduling [3,4], demand

☆ This work was supported in part by the Coordenação de Aperfeiçoamento de Pessoal de Nível Superior (CAPES), Brazil, Finance Code 001 and by the Fundação de Amparo à Pesquisa do Estado de São Paulo (FAPESP), Project 2024/03306-8.

* Corresponding author.
Email addresses: manassero@usp.br (G. Manassero Jr.), rodrigo.tiferes@usp.br (R.R. Tiferes), thamiris@usp.br (T.N. Ribeiro), andrea.mazza@polito.it (A. Mazza), enrico.pons@polito.it (E. Pons).

https://doi.org/10.1016/j.apenergy.2026.128351
Received 10 April 2026; Received in revised form 2 June 2026; Accepted 30 June 2026
Available online 3 July 2026
0306-2619/© 2026 The Author(s). Published by Elsevier Ltd. This is an open access article under the CC BY license (http://creativecommons.org/licenses/by/4.0/).

Table 1
Comparison of related works on data center allocation and hosting capacity and resilience analysis.

Reference	Grid Level†	Existing grid constraints	Assumes grid expansion	Data center scale	Multi-contingency	Resilience assessment	Objective‡
[8]	D	Yes	No	≤ 100 MW	No	No	CM
[17]	T	No	Yes	GW-scale	No	No	RS
[18]	T	No	Yes	GW-scale	No	No	RS
[19]	T	Yes	No	≤ 100 MW	Partial	Limited	CM
[20]	D	Yes	No	≤ 100 MW	No	No	CM
[21]	D	Yes	No	≤ 100 MW	No	No	CM
[22]	D	Yes	No	≤ 100 MW	No	No	CM
[23]	D	Yes	No	≤ 100 MW	No	No	CM
[24]	D	Yes	No	≤ 100 MW	No	No	CM
[25]	D	Yes	No	≤ 100 MW	No	No	CM
[26]	D	Yes	No	≤ 100 MW	No	No	CM
[27]	D	Yes	No	≤ 100 MW	No	No	CM
This work	T	Yes	Yes⋆	GW-scale	Yes	Yes	CM and RS

† D: distribution level; T: transmission level. ‡ CM: hosting capacity maximization; RS: region selection. ⋆ If the expansion plan is available.

response [5,6], use of energy storage and renewable sources [7,8], waste heat recovery [9,10], carbon neutral cloud services [11], among others [12,13]. However, for transmission planning purposes, the data centers' maximum power demands must be considered to analyze the grid's behavior under the most critical conditions, and as concluded in the IEEE Power & Energy Society's report on data center growth and grid readiness (May 2025) [14], most existing transmission systems are not capable of suddenly accommodating such large loads. Hence, in many cases, the construction of a new large-scale data center may be severely delayed or even prohibited because new transmission infrastructure must be built (which, on the other hand, entails additional and notable carbon emissions [15,16] and increases costs to all of society).

In this context, proposing analytical tools and application studies that demonstrate how to allocate and construct new large-scale data centers on an existing transmission network, while simultaneously accommodating the maximum data center capacity and minimizing, or even eliminating, the need for additional infrastructure, is key to meeting the demand expected in the upcoming years.

1.2. Literature review

The current literature includes diverse studies addressing optimal data center expansion plans. For instance, reference [17] proposes an expansion scheme to identify optimal regions for constructing new carbon-neutral data centers by balancing costs, access to local clean energy, and regional incentive policies. Complementarily, Wang et al. [18] present a bi-objective optimization model to select the most appropriate location for new data centers, considering both expansion costs and the carbon emissions associated with energy use.

Reference [19] presents an expansion planning framework for data centers and data routes aimed at ensuring acceptable service rates to end users in the data network. It determines the location and capacity of data centers as well as the necessary data routes while accounting for constraints imposed by both the power and data networks, i.e., it acknowledges the grid's limited capacity and does not involve building new infrastructure. Similarly, Guo et al. [8] propose an optimization-based planning scheme that uses a Multi-Objective Natural Aggregation Algorithm to determine the locations and capacities of interconnected internet data centers and battery energy storage systems in a smart distribution grid. Their model also respects the existing grid's limitations and avoids new construction. Reference [20] proposes a planning model for data centers and distribution networks that incorporates demand response and multivariate uncertainties. Reference [21] describes an optimal planning method for regional integrated electricity-heat systems with data centers, considering wind power uncertainty. The authors of Wu et al. [22], in turn, account for spatial-temporal flexible resources and multi-network coupling to propose a cyber-physical integrated planning model for the distribution network, which also includes internet data centers. Complementarily, reference [23] proposes a joint expansion planning approach for distribution systems considering both internet data centers and electric vehicle charging stations.

The authors of Ma et al. [24], then, propose an optimized planning methodology to allocate data centers within integrated multi-energy microgrids, combining renewable sources and low-carbon technologies to make data center operation more sustainable, economical, and resilient to uncertainty. In turn, Zhang et al. [25] present a multi-objective interval optimization method for expansion planning in active distribution systems with distributed internet data centers and renewable generation. Along the same lines, Su et al. [26] propose a collaborative planning framework for distribution networks, data centers, and renewables via interval optimization. Complementarily, Wang et al. [27] propose a robust planning model to define the ideal structure of a data center park, considering location, integration with photovoltaic generation, energy storage, and flexible substations. This model contributes to efficient resource allocation and data center siting by optimizing both operational economy and reliability, even under uncertainties such as load and generation variations.

1.3. Research gap

Recent studies on data center planning and allocation have addressed various aspects of the problem, yet no unified framework currently captures all the technical and operational requirements of modern large-scale deployments. A structured comparison of the main characteristics of these approaches is provided in Table 1, where the research gap is clearly identified across the considered approaches.

First, a significant portion of the literature is developed at the distribution or sub-transmission level, which inherently limits the admissible load size and does not reflect the requirements of modern large-scale data centers, typically ranging from several hundred megawatts to gigawatt-level capacities. Therefore, these large-scale facilities, can only be realistically accommodated at the transmission level.

Second, while some approaches account for grid constraints, others implicitly assume that new transmission infrastructure will be deployed to support the integration of data centers. Such an assumption may not be suitable for scenarios requiring rapid deployment, as transmission expansion typically involves long lead times and additional environmental impacts. Therefore, practical planning requires assessing the hosting capacity of the existing transmission grid based solely on its current configuration.

Third, the scale of the data centers considered in many studies is not representative of current industrial trends, i.e., utility-scale data

centers. Most works focus on relatively small installations, whereas contemporary data centers demand substantially higher power levels, reinforcing the need for transmission-level analyses.

Fourth, most existing methods do not explicitly account for multiple contingency scenarios in the grid. This limitation is important, as large data centers constitute critical and highly sensitive loads whose operation must remain robust under adverse system conditions. Ensuring that candidate locations do not lead to severe operational consequences under contingencies is therefore a fundamental requirement.

Fifth, even when contingency analysis is partially included, the concept of resilience is often not explicitly addressed. In this context, resilience encompasses both the grid's ability to withstand disturbances and the data center's capacity to maintain operation under such conditions.

Finally, existing studies typically focus either on identifying geographically suitable regions or on maximizing hosting capacity, but rarely integrate both perspectives within a consistent transmission-level framework with realistic load sizes and operational security requirements.

In light of these limitations, a clear research gap emerges. Data centers are becoming critical infrastructure for cloud services, digital platforms, and AI-based applications. In particular, the rapid growth of AI workloads has intensified demand for large-scale facilities with power requirements ranging from hundreds of megawatts to gigawatts. At the same time, the economic viability of these projects depends heavily on short deployment timelines, making it essential to identify locations where large loads can be connected securely and within the available hosting capacity of the existing transmission network. However, to the best of the authors' knowledge, there is currently no methodology that simultaneously (i) operates at the transmission level, enabling realistic large-scale data center integration, (ii) respects the constraints of the existing grid without assuming prior network expansion, (iii) considers data center capacities in the order of hundreds of megawatts to gigawatts, and (iv) explicitly evaluates system performance under multiple contingency scenarios while assessing resilience, and addressing this gap is necessary to enable the secure and timely integration of large-scale data centers into transmission networks.

1.4. Contribution

In this context, this research intends to contribute to the identified gap by proposing a methodology to support the optimal allocation of new large-scale data centers within transmission grids, while respecting the available hosting capacity of the existing infrastructure and ensuring resilience to multiple contingencies (as in Table 1).

The proposed framework addresses the identification of optimal locations for large-scale data center integration, subject to the explicit constraint that the existing transmission infrastructure must be sufficient to accommodate the new demand. This premise reflects practical planning constraints, including substantial investment requirements, lengthy permitting and construction timelines, and additional environmental impacts associated with infrastructure expansion. Moreover, the implementation schedule of new transmission assets or network reinforcements may be incompatible with the faster deployment timeline of large-scale data centers, potentially leading to project delays, financial losses, and uncertainty for investors, developers, and utilities.

The proposed method focuses on hosting capacity and siting optimization within the current grid, using steady-state power flow, voltage limits, losses, and contingency criteria as the main screening indicators adopted in transmission planning studies to assess network adequacy under critical operating conditions. Data center capacity is included in the optimization formulation, allowing the method to evaluate where data centers can be connected and how much demand can be hosted at each candidate location without requiring additional grid reinforcements.

The methodology identifies data center allocations that remain technically feasible across a defined set of contingency scenarios. By jointly addressing hosting capacity limits and operational resilience, the proposed approach supports the placement of data centers within the existing transmission infrastructure, without requiring new transmission assets or additional grid reinforcements. This aspect is increasingly relevant in the context of climate change, where extreme rainfall or wind events may cause simultaneous outages of multiple transmission components [28–31].

1.5. Article structure

The next sections are organized as follows: Section 2 presents and describes the proposed methodology; Section 3 shows a case study in which this methodological framework was used in a real transmission network; Section 4 presents the corresponding results; and Section 5 concludes this work.

2. Methodology

The methodology proposed in this work is based on an optimization procedure for allocating data centers within a region of interest in a high-voltage power transmission system. The method employs the heuristic technique Particle Swarm Optimization (PSO), whose main objective is to minimize transmission losses in that region while simultaneously ensuring: (i) that voltage profiles remain close to the nominal values; (ii) that multiple data center allocations do not occur at the same node before all feasible nodes have been allocated, considering that the number of available bays in existing substations is limited and that new expansions are generally the exclusive responsibility of each data center developer, not shared with other developers; and (iii) that currents in the equipment within the region of interest (transmission lines, transformers, and other transmission components) remain below the rated or overload current limits specified in the design.

PSO is a heuristic method inspired by collective swarm behavior, such as flocks of birds or schools of fish. Each candidate solution is treated as a "particle" that moves throughout the search space influenced by two components: its own best historical position (cognitive component) and the best position found by the swarm (social component) [32]. In this work, each candidate solution is represented by an integer (for a single allocation) or a set of integers (for multiple allocations), indicating the nodes (substation buses and/or possible line tappings) in the region of interest where data centers may be sited. This technique ensures that the search process operates directly over the feasible physical locations. The iterative update of particle positions allows the method to efficiently explore the search space and converge toward promising regions without requiring gradients or other analytical properties of the objective function. This stochastic and cooperative nature makes PSO particularly suitable for complex optimization problems with multiple constraints.

The proposed methodology is described in detail in this section. First, an overview of the optimization framework and the underlying principles of the PSO technique is presented. Subsequently, the formulation of the objective function and its individual components is introduced, followed by the procedures used for hosting capacity assessment, optimal data center allocation, and contingency testing aimed at evaluating system resilience.

2.1. Proposed framework overview

The methodology is based on electrical calculations of the region of interest, incorporating the proposed data center allocations. This calculation yields losses, voltage profiles, and equipment currents. For this purpose, the Alternative Transients Program (ATP) software was used. ATP is widely employed for power system analyses, especially those involving transient phenomena. However, before any simulation is executed, ATP performs a steady-state calculation known as the pre-fault solution. This calculation is mathematically equivalent to a simplified load-flow solution, without iterative generation dispatch

and automatic voltage regulation. As a result, ATP provides nodal voltages, power flows, and currents consistent with the specified operating point, enabling its use as a steady-state calculation tool in the proposed methodology. ATP was chosen arbitrarily, and any other similar program could be used for the same purpose. Additionally, a purpose-built power-flow routine based on assembling the nodal admittance matrix could have been implemented without loss of generality or accuracy.

Initially, the methodology consists of preparing a template file in ATP containing the electrical network of the region of interest, including all loads already present in that network, as well as any operating data centers, but excluding the new data centers to be allocated. This file consists of all buses in the area of interest, the Thévenin equivalents representing coupling with the remainder of the bulk power system, and all possible line tappings.

The template consists of the *per-unit* (pu) positive-sequence electrical system. The transmission lines (TLs) are represented using the π-equivalent model. The transformers (XFMRs) are represented, neglecting the magnetizing branch. The Thévenin equivalents of the interface buses between the region of interest and the remainder of the bulk power system are modeled as ideal voltage sources in series with positive-sequence impedances that represent the fault levels at those buses. Loads are modeled as constant impedances, including both existing data centers and those to be allocated. This choice derives from the simplicity of representing such a model in ATP. However, any load model that more accurately represents the electrical behavior of the data centers could have been adopted without loss of generality. The magnitudes and angles of the voltage sources must reflect the power flow at the instant for which the optimal data center allocation is selected, and the data center loads must reflect their power at that same instant, which may even be less than their maximum.

Evidently, throughout the day, the data centers' loads vary, as well as the magnitudes and angles of the equivalent sources. Nevertheless, the worst-case scenario was selected, namely when data centers operate at maximum power, and the region of interest is already heavily loaded. Naturally, the proposed methodology may be applied to any chosen load model and operating scenario. Selecting the worst case is motivated by the need to evaluate whether the network planning horizon is adequate given the expected volume of new connection requests from data centers in the future.

From the template file, the methodology generates a new file by adding the data centers to the nodes selected by the PSO, with their respective powers and power factors. The ATP executable is then launched, performing the simulation and producing an output file containing the load flow results. The relevant values are extracted from this file: losses in all network branches, nodal voltages at all buses, and branch currents in transmission equipment. These results serve as inputs to the computation of the PSO objective function, which is composed of the four components described next.

It is also important to point out that in this implementation, ATP is used as the external electrical network analysis tool responsible for the power-flow calculation. Therefore, the selected load model and power factor influence only the ATP simulation results, without changing the formulation of the optimization method. As a result, the proposed method can be applied with different load models (e.g., constant power) and power factors, and ATP could also be replaced by another power-flow calculation tool without modifying the structure of the proposed optimization framework.

2.2. Objective function formulation

The objective function combines performance metrics and penalty terms for constraints into a single scalar value to be minimized by the PSO algorithm. It comprises four components, each designed to capture a distinct aspect of system performance and operational feasibility within the existing transmission infrastructure. Network losses are used to favor allocations that impose lower additional stress on the grid.

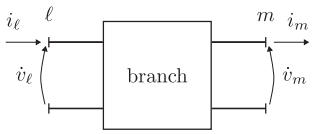


Fig. 1. Complex power per branch.

Voltage deviations are considered to ensure that the new data center demand can be accommodated without compromising voltage adequacy. Current violations explicitly penalize allocations that exceed the loading limits of existing transmission equipment, thereby preventing solutions that would implicitly require line or transformer reinforcement. Finally, repeated node allocation penalizes the concentration of multiple data centers at the same bus. This is relevant because existing substations have limited available bays, and allocating several large loads to the same substation could require additional bay construction or substation expansion. Therefore, these terms help preserve the solution's practical feasibility within the existing transmission infrastructure.

Each component of the objective function is multiplied by a weighting factor to make the four terms comparable in magnitude. These factors were selected through manual tuning to balance the contributions of the four components and avoid an optimization process driven predominantly by a single term. This scaling procedure ensures that losses, voltage deviations, current violations, and repeated node allocations all contribute effectively to the search for feasible, technically suitable data center allocations. The individual components of the objective function are described in detail in the following subsections.

2.2.1. First component

The first component corresponds to the sum of the electrical losses in the transmission network branches located within the region of interest. Only internal losses are computed, disregarding both the power supplied by the Thévenin equivalents and the power consumed by all loads in the system (including existing and newly allocated data centers). Hence, this component represents exclusively the losses associated with energy transport within the network, directly reflecting the impact of data center allocation on its electrical performance. According to Fig. 1, the complex power lost within the k-th branch, $\bar{s}_k$, in pu, is given as

$$\bar{s}_k = \bar{s}_{\ell,m} = \dot{v}_\ell \cdot i_\ell^* - \dot{v}_m \cdot i_m^* \tag{1}$$

where k is the k-th branch delimited by nodes ℓ and m; $\dot{v}_\ell$ and $\dot{v}_m$ are the node voltages, in pu, of ℓ and m nodes, respectively; and i_ℓ and i_m are the injected node currents, in pu, in the same nodes. Considering that the number of branches is n_b, the total complex power lost in the region of interest transmission branches, $\bar{s}_{\text{losses}}$, in pu, is

$$\bar{s}_{\text{losses}} = \sum_{k=1}^{n_b} \bar{s}_k \tag{2}$$

and the first component of the objective function, f_1, is

$$f_1 = \Re\left\{\bar{s}_{\text{losses}}\right\} \tag{3}$$

2.2.2. Second component

The second component is a penalty applied whenever nodal voltages within the region of interest violate the admissible upper or lower limits. This component ensures that solutions producing excessively high or low voltages are discouraged, favoring configurations that maintain voltage profiles near nominal. It depends on individual penalties assigned to each node voltage magnitude v_j based on its deviation from a predefined

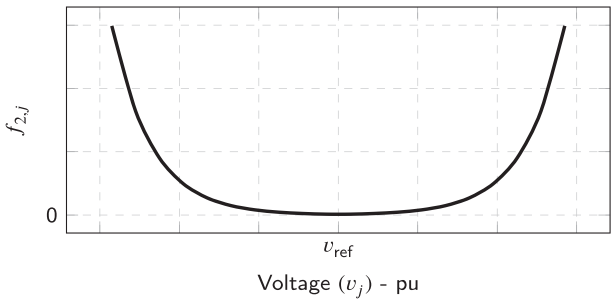


Fig. 2. Individual node voltage violation penalty.

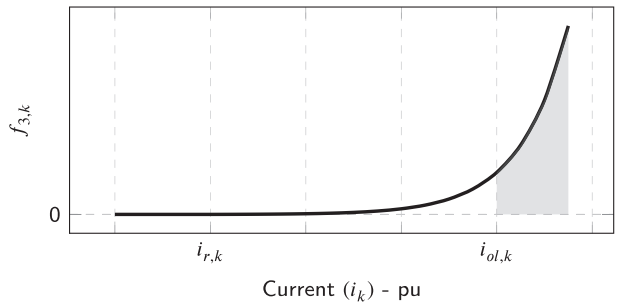


Fig. 3. Individual branch current violation penalty.

reference value v_{ref}, as in

$$f_{2,j} = \mathrm{e}^{\frac{|v_j - v_{\text{ref}}|}{\alpha}} - 1 \tag{4}$$

where $j = \{1, \ldots, n\}$; n is the total number of nodes; and α is a weighting factor used to scale $f_{2,j}$ according to the magnitude of f_1. Fig. 2 illustrates the behavior of this penalty. The second component is defined as the average of the sum of all individual terms, as in

$$f_2 = \frac{1}{n} \cdot \sum_{j=1}^{n} f_{2,j} \tag{5}$$

2.2.3. Third component

The third component is also a penalty, now associated with violations of the transmission equipment current limits within the region of interest. When the rated current limit is exceeded, a penalty of magnitude comparable to those of the previous two components is applied, thereby preserving balance in the objective function. However, if the solution violates the maximum overload current limit, which is an inadmissible condition that would require mandatory reinforcements by the transmission utility, a significantly more severe penalty is applied. It depends on individual penalties assigned to each branch's current magnitude i_k based on its deviation from a predefined reference value $i_{r,k}$ as in

$$f_{3,k} = \mathrm{e}^{\frac{|i_k - i_{r,k}|}{\beta \cdot i_{r,k}}} - 1 \tag{6}$$

where $k = \{1, \ldots, n_b\}$, n_b is the total number of branches, and β is a weighting factor used to scale $f_{3,k}$ according to the magnitude of f_1. For current values i_k up to the rated current threshold $i_{r,k}$, the contribution of $f_{3,k}$ remains limited, whereas for i_k exceeding the overload current threshold $i_{ol,k}$ the penalty increases sharply, highlighting the critical importance of this condition. Fig. 3 illustrates the behavior of this penalty. In this figure, the transparent region represents the penalty associated with currents exceeding the rated design current. In turn, the gray region indicates the penalty applied when the current exceeds the maximum allowable overload current.

The third component of the objective function is then defined as the sum of all individual terms, as in

$$f_3 = \sum_{k=1}^{n_b} f_{3,k} \tag{7}$$

2.2.4. Fourth component

The fourth component of the objective function introduces an additional penalty that accounts for the physical limitation of allocating more than one data center to the same node (bus or line tapping) within the region of interest. In practice, the number of available bays in existing substations is limited, and substation expansions are typically performed individually by each data center developer, rather than being shared among multiple companies. If the number of buses is fewer than the total number of data centers to be allocated, this condition must not prevent the optimization from converging. Accordingly, a progressive penalization strategy is adopted to discourage the simultaneous allocation of two or more data centers to the same node, while preserving the robustness of the iterative PSO process and maintaining the general applicability of the proposed methodology.

For each node let d_j denote the number of data centers allocated to that node. A conditional penalty is applied only when multiple allocations occur at the same node. Specifically, if $d_j > 1$, a penalty proportional to the number of allocated data centers is introduced through a weighting factor γ; otherwise, no penalty is imposed. Eq. (8) describes the proposed penalty per node.

$$f_{4,j} = \begin{cases} \gamma\, d_j, & \text{if } d_j > 1, \\ 0, & \text{otherwise.} \end{cases} \tag{8}$$

where γ is also a weighting factor used to scale $f_{4,j}$ according to the magnitude of f_1.

The fourth component of the objective function is, therefore, defined as the sum of all individual terms, as in

$$f_4 = \sum_{j=1}^{n} f_{4,j} \tag{9}$$

2.2.5. Objective function

Finally, the objective function to be minimized is the sum of the four components, as shown in

$$f = f_1 + f_2 + f_3 + f_4 \tag{10}$$

2.3. Applications of the proposed methodology

After defining the optimization framework and the objective function, the proposed methodology is applied to address practical planning and operational questions related to the integration of large-scale data centers. In particular, the methodology is employed to assess the hosting capacity of the area of interest, determine the optimal allocation of a selected number of data centers, and evaluate the robustness of the resulting solutions through contingency analysis. These applications demonstrate how the same optimization framework can be used to support different stages of transmission system planning and operational assessment.

2.3.1. Hosting capacity assessment

The methodology proposed in this work begins with an assessment of the region of interest's hosting capacity. Hosting capacity refers to the maximum number of data centers that can be integrated into the

area without violating operational constraints, specifically the overload-current limit. To determine this capacity, an outer iterative procedure is employed within the optimization framework. During each iteration, an additional data center is added to the initial set of units considered for allocation. The optimization problem is then solved again based on the updated loading scenario. This process continues until the system reaches a condition in which the overload-current limit is exceeded. At this point, the hosting capacity is identified as the maximum number of data centers that can be integrated without violating this operational constraint.

In the proposed formulation, each newly added data center is assumed to have an identical power rating. This assumption simplifies the characterization of hosting capacity without compromising the generality of the methodology. The framework can be readily adapted to accommodate uneven load increments or finer adjustments to the power ratings of successive data centers, thereby enabling incremental assessment of hosting capacity when required. Moreover, the worst-case operating condition is adopted to determine the hosting capacity; however, the methodology is fully applicable to any alternative operating scenario of interest.

2.3.2. PSO-based optimal data center allocation

After the hosting capacity of the area of interest has been determined, the methodology proceeds with the optimal allocation of data centers based on the selected number of units to be connected. This allocation is obtained through the previously described optimization process, which identifies the most suitable buses within the area of interest while respecting all operational constraints. Once the optimal locations have been defined, the resulting configuration serves as the basis for the subsequent contingency analysis, in which the system is evaluated under degraded operating conditions to assess the network's resilience with respect to the newly allocated data centers.

2.3.3. Contingency testing

After the optimal data center allocation is obtained, a contingency analysis is performed to assess the resilience of the resulting solution. In this step, selected contingencies affecting the region of interest are simulated in ATP by modifying the original template file to remove the equipment assumed to be out of service in the contingency under analysis, such as transmission lines, transformers, or sectionalizing devices that connect the area of interest to the remainder of the bulk power system. After this modification, the methodology proceeds to include the optimally allocated data centers at the nodes determined by the PSO solution. For each contingency scenario, ATP executes a new steady-state (pre-fault) calculation, providing nodal voltages, branch currents, and power flows under the degraded operating condition. The objective of this analysis is to verify that the allocated data centers remain connected without violating voltage or rated or overload current limits, and to identify contingencies that may compromise system resilience. This procedure enables the evaluation of the network's ability to accommodate new data centers not only under normal operating conditions, but also under credible contingencies, thereby providing a quantitative assessment of the operational resilience of the proposed allocation.

Finally, to illustrate the proposed methodology, Fig. 4 presents the conceptual block diagram of the adopted approach. The diagram summarizes the main stages of the method, from the prior definition of the region of interest and the generation of the ATP template, through the hosting capacity assessment and the PSO-based optimal allocation of data centers, to the final contingency analysis to evaluate system resilience. This representation highlights the interaction between the outer hosting capacity evaluation loop and the inner optimization process, as well as the role of ATP's steady-state calculations in supporting each step.

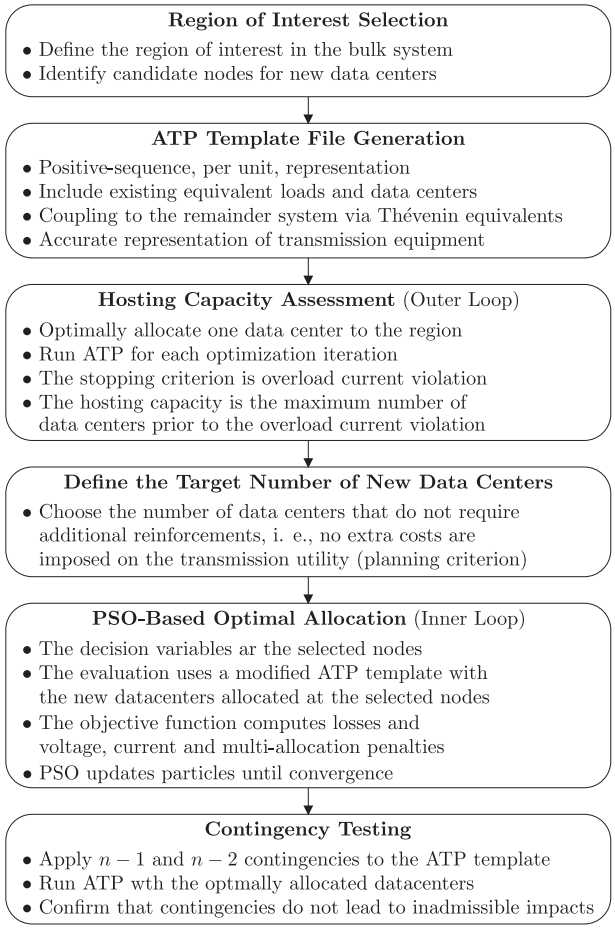


Fig. 4. Block diagram of the proposed methodology.

3. Case study

This section presents a case study illustrating the application of the methodology to a real transmission grid.

3.1. Transmission system of the region of interest

The Brazilian interconnected power system is continental in size, currently comprising ≈ 240 GW of generation capacity and a transmission grid exceeding 170,000 kilometers. Within this system, the state of São Paulo hosts the largest concentration of transmission facilities [33], and its grid does have some large-scale data centers already in commercial operation, in a region encompassing São Paulo city and nearby urban areas that contain appropriate communications infrastructure.

In recent years, the transmission companies responsible for this region have received numerous requests to connect new data centers at various locations (some within existing substations and others at potential tapping points along the existing lines). However, in most cases, the data center developers request connections for loads approaching GW capacity at locations where the system may not be able to accommodate them without the construction of significant additional infrastructure. Moreover, utilities and the Brazilian Transmission System Operator may be slow to respond to connection requests because the grid nodes' capacity to host new large-scale data center loads has not yet been mapped.

In this context, the methodology developed in this research was applied to the São Paulo region with the highest demand for new data center connections. This way, please refer to Fig. 5, which illustrates the transmission grid in this region, which has seven operating data

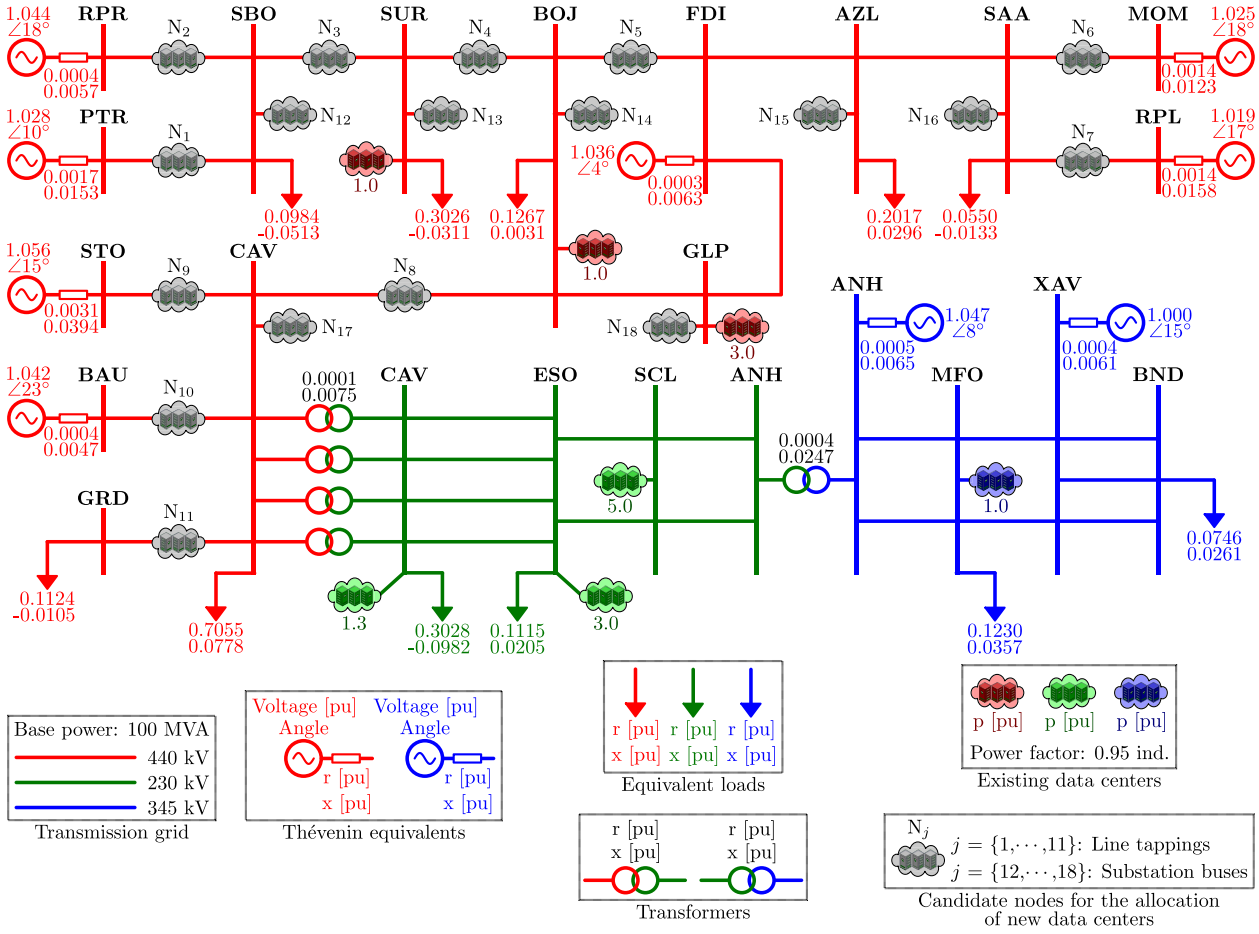


Fig. 5. Transmission grid considered in this case study, with eighteen candidate nodes for the allocation of new data centers.

centers and eighteen candidate nodes for potential new data center allocations (N_1, ⋯, N_{18}). Please notice that the figure also displays the values corresponding to the Thévenin equivalents and the equivalent loads, which reflect the impact of the studied system's connection to the larger Brazilian grid. These values were obtained from official databases provided by Brazil's Energy Research Office and correspond to a critical loading condition projected for 2030, when the new data centers currently planned are expected to be constructed. As mentioned earlier, the proposed methodology can be applied to various scenarios; however, the most critical scenario is the one that must be considered to assess the grid's hosting capacity, determine optimal data center allocations within the candidate nodes, and analyze the resilience of each allocation under contingencies.

Additionally, please refer to Table 2, which presents the rated and overload currents, along with the resistance, reactance, and susceptance parameters for each line in the network, in *per-unit* (pu) values. All candidate nodes of the potential line tapping type are located in the middle of their respective lines, except for N_{10}, whose distance from CAV corresponds to 20% of the total length of the CAV-BAU line. Furthermore, please consider that the rated and overload currents of the CAV substation transformers (440/230-kV) are 7.50 and 7.96 pu, while these capacities for the transformer in substation ANH (345/230-kV) are 10 and 12 pu. Furthermore, the maximum current that the Thévenin equivalents can supply, based on the actual system data, is 95 pu for BAU, 50 pu for RPR and FDI, 45 pu for ANH and XAV, and 15 pu for PTR, STO, RPL, and MOM.

With all the parameters for the transmission network in the region of interest, the pu and single-phase equivalent circuit of the system were then modeled in the ATP.

Table 2
Parameters of the transmission lines.

From	To	$i_{r,k}$	$i_{ol,k}$	r	x	y
RPR	SBO	15.2	15.2	0.0022	0.0303	1.6337
PTR	SBO	15.2	15.2	0.0003	0.0039	0.2259
SBO	SUR	15.2	15.2	0.0003	0.0034	0.1921
SUR	BOJ	15.2	15.2	0.0006	0.0080	0.4581
BOJ	FDI	20.3	20.3	0.0009	0.0097	0.5815
FDI	AZL	20.3	20.3	0.0008	0.0098	0.6006
AZL	SAA	15.2	15.2	0.0006	0.0081	0.4872
SAA	MOM	15.2	15.2	0.0023	0.0288	1.8557
SAA	RPL	15.2	15.2	0.0018	0.0219	1.4196
FDI	GLP	20.3	20.3	0.0006	0.0075	0.5000
GLP	BOJ	20.3	20.3	0.0006	0.0075	0.5000
BOJ	CAV	20.3	24.5	0.0003	0.0038	0.2371
CAV	STO	15.2	15.2	0.0002	0.0023	0.1360
CAV	BAU	15.2	15.2	0.0030	0.0376	2.4206
CAV	GRD	15.2	15.2	0.0003	0.0031	0.1851
CAV	ESO	5.00	6.00	0.0030	0.0220	0.0801
ESO	SCL	5.00	6.00	0.0005	0.0028	0.0095
SCL	ANH	5.00	6.00	0.0014	0.0079	0.0265
ANH	MFO	17.9	17.9	0.0001	0.0023	0.0361
MFO	XAV	11.9	11.9	0.0002	0.0038	0.1061
XAV	BND	5.00	6.00	0.0001	0.0018	1.1684

3.2. Objective function component parameters

Before moving to the results, it is also important to state which parameters were used for computing the f_2, f_3, and f_4 components of the objective function. Thus, for the calculation of f_2, $v_{\text{ref}} = 1.00$ pu and $\alpha = 0.10$ were chosen. For the calculation of f_2, the values of $i_{r,k}$ and $i_{ol,k}$ presented in Table 2 (and those mentioned for the transformers and

Thévenin equivalents) and $\beta = 0.05$ were used. Finally, for the calculation of f_4, $\gamma = 10$ was chosen. It is worth noting that these values for α, β, and γ were manually tuned to maintain comparability among the four components of the objective function, but that others could be used instead if deemed of interest by the methodology's user.

4. Results

This section presents the results obtained by applying the proposed methodology to the selected region of interest within the transmission network. The results are organized according to the main stages of the method and aim to demonstrate its practical applicability and consistency.

First, the region's hosting capacity is assessed through an incremental allocation process. Next, the optimal allocation of data centers is determined based on the identified hosting capacity. Finally, contingency analyses are conducted to evaluate the operational robustness and resilience of the resulting allocations under degraded operating conditions.

4.1. Hosting capacity assessment

The hosting capacity assessment was conducted according to the methodology described in Section 2. For this purpose, a nominal power of 100 MW per data center was adopted, with a power factor of 0.95, and used as the basic increment in the hosting capacity evaluation. This fixed power level was selected to represent large-scale data center installations and to allow a clear interpretation of the incremental loading effects on the transmission network.

The hosting capacity was evaluated using two distinct approaches. In the first approach, a brute-force allocation was performed, testing all feasible combinations of data center placements within the region of interest. In the second approach, the same problem was solved using the previously described PSO-based optimization framework. The adoption of both approaches aimed to verify whether the PSO algorithm consistently converges to the global minimum of the objective function rather than being trapped in local minima.

The comparison between brute-force and PSO-based results enabled a careful calibration of the PSO parameters. In particular, the swarm size was set to 10 particles, randomly initialized among the 18 candidate nodes of the region of interest, without repetition, ensuring that each particle represented a physically feasible allocation. The observation of convergence behavior and solution consistency across multiple runs guided these adjustments.

Both brute-force simulations and PSO-based optimization produced identical results for hosting capacity, confirming that the PSO formulation and parameterization correctly identified the global solution. Moreover, the total execution times of the two approaches were also comparable. This behavior is explained by the incremental nature of the hosting capacity assessment, in which the computational effort is dominated by successive steady-state simulations rather than by the search strategy itself. It should be noted that the main computational bottleneck of the hosting capacity assessment does not stem from the optimization algorithm. Instead, it arises from the interaction between the Matlab control script, the file I/O operations required to write and read ATP input and output files, and the system calls used to invoke the ATP executable. As a consequence, the overall execution time is primarily governed by external simulation overheads, making the relative cost of brute-force and PSO-based approaches similar in this specific application.

The hosting capacity assessment was conducted over a maximum allocation horizon of 10 GW of total data center power. Although such a power level inevitably leads to overload-current violations, this extended range was intentionally explored to analyze the behavior of the objective function components beyond the feasible operating region. Fig. 6 illustrates the evolution of the objective function components

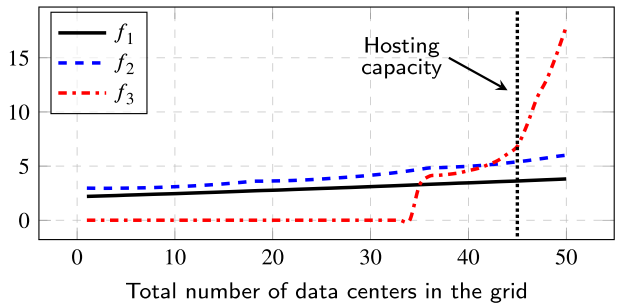


Fig. 6. Objective function components' behavior during hosting capacity assessment (f_1 given in pu; f_2 and f_3 are dimensionless).

Table 3
Three-load sets used for the optimal allocation tests.

Load	Load (MW)			Total
Set	1	2	3	(MW)
Set 1	3000	450	1200	4650
Set 2	2100	450	2250	4800
Set 3	1350	1500	1650	4500

f_1 (transmission losses), f_2 (voltage-related penalties), and f_3 (current-related penalties) as the total allocated data center power increases. The fourth component, f_4, is not shown because it corresponds to a discrete penalty for multiple allocations at the same node and increases monotonically whenever such a condition occurs. As observed in Fig. 6, the current-related component f_3, which represents the most critical operational constraint, begins to increase sharply at approximately 4.5 GW of total allocated power. From this behavior, it can be inferred that the hosting capacity of the region of interest is approximately this value.

4.2. Optimal data center allocation

After determining the hosting capacity, as described in the previous subsection, and verifying that the PSO-based methodology consistently converged to the global minimum, the optimal allocation problem was further addressed. To this end, three distinct sets of three data center loads were defined and each individual set was optimally allocated using the original ATP template. Each load set was analyzed independently to assess the behavior of the optimization process and its sensitivity to different loading distributions.

Only three sets of three loads were considered at this stage to keep the computational burden of a brute-force search within reasonable limits. This choice enabled a direct comparison between brute-force enumeration and PSO-based optimization, ensuring that the latter converged to the global minimum in all tested cases.

The three load sets are listed in Table 3. The individual load values were selected to achieve a total power close to the previously identified hosting capacity, and all loads were modeled with a power factor of 0.95.

For these tests, the initial PSO swarm consisted of a random sample of 50 particles, each representing a feasible allocation solution without repetition. Considering that the total number of possible allocation combinations is $18^3 = 5832$, this initial swarm corresponds to approximately 0.86% of the complete solution space. The same initial swarm was used for all three load sets to evaluate whether swarm initialization would affect optimization results in terms of accuracy or convergence speed.

The comparison between brute-force enumeration results and PSO results showed that the PSO algorithm converged to the global minimum for all three load sets. The optimal node allocations identified for each load set are summarized in Table 4, together with the corresponding values of the first three components of the objective function. The fourth

Table 4
Optimal node allocation for the three-load sets.

Load	Node			Components		
Set	1	2	3	f_1	f_2	f_3
Set 1	N_{16}	N_2	N_{12}	3.88	4.67	0.0
Set 2	N_5	N_2	N_{16}	3.79	4.95	0.0
Set 3	N_1	N_{15}	N_{16}	3.80	4.70	0.0

component is zero for all cases, since the optimal allocation assigns three loads to distinct buses among the 18 available candidates. It can be observed that the third component, which represents the most critical constraint, is also zero for all three optimal allocations, as expected given the higher penalization associated with violations of current limits in the objective function formulation.

The total execution times of the brute-force and PSO-based simulations were also comparable in these cases, for the same reasons discussed in the hosting capacity assessment: the dominance of steady-state simulations and external file-handling operations over the optimization process itself.

To further investigate the convergence properties of the PSO algorithm, an additional test was conducted using a reduced swarm size. Specifically, only the first 10 particles from the original swarm of 50 were retained, and the optimization was repeated for the last load set. Convergence to the global minimum was again observed; however, the convergence time increased by approximately 16%, indicating a trade-off between swarm size and convergence speed.

After completing the tests with three-load sets, an additional scenario involving a single set of four loads was analyzed. All four loads were modeled with a power factor of 0.95 and individual powers of 900, 600, 1200, and 1800 MW, for a total of 4500 MW. For this case, a brute-force search was again performed. However, the total simulation time exceeded 8 hours, given that the search space comprises $18^4 = 104{,}976$ possible allocation combinations. In contrast, the PSO-based approach was configured with 1500 particles, corresponding to approximately 1.43% of the total solution space, and converged to the same global minimum in approximately 4 hours. This result demonstrates a clear computational advantage of the PSO-based optimization over brute-force enumeration as the dimensionality of the allocation problem increases.

In this four-load scenario, both approaches identified the same optimal allocation, placing the loads on candidate nodes N_2, N_1, N_6, and N_5, respectively. The corresponding values of the first three components of the objective function are $f_1 = 3.55$, $f_2 = 4.43$, and $f_3 = 0.0$, indicating that the optimal solution does not lead to violations of the most critical current-related constraint.

4.3. Contingency testing and resilience assessment

The contingency testing was performed using the three optimally allocated three-load sets and the optimally allocated four-load set obtained in the previous subsection. These configurations were selected to evaluate the robustness and resilience of the proposed allocation methodology under degraded operating conditions affecting the transmission network. To this end, a set of modified ATP template files was created to represent different contingency scenarios in the network illustrated in Fig. 5. First, ten new ATP templates were generated considering single-contingency ($n-1$) events. In each of these cases, the contingency consisted of removing a single network element, such as a transmission line or transformer, from the original template. In addition, five new ATP templates were created to represent double-contingency ($n-2$) events, in which two network elements were simultaneously removed from service.

The contingencies were randomly selected from a total of 45 possible network elements in the system shown in Fig. 5. The complete list of $n-1$ and $n-2$ contingencies considered in this study is presented in Tables 5 and 6. With respect to the contingency testing, particular attention should be given to the outage of the 345/230-kV transformer under the $n-1$ scenario. This contingency is especially relevant because it electrically separates the network depicted in Fig. 5 into two distinct subsystems, significantly altering the power-transfer paths between voltage levels. As a result, new current flow patterns are imposed on both remaining circuits, leading to a redistribution of power that directly affects line loadings and voltage profiles within the region of interest. In addition, two of the $n-2$ contingency scenarios involve the disconnection of a transmission line between nodes XAV and BND. These contingencies are also significant, since this network section was already heavily loaded before the allocation of the new data centers. The simultaneous removal of this corridor with another network element, therefore, represents a critical stress condition for the system, making it especially suitable for evaluating the resilience of the optimal allocation under severe operating scenarios.

Table 5
$n-1$ contingency scenarios.

No.	From	To	Equipment
1	N_3	SUR	TL
2	BAU	N_{10}	TL
3	CAV	CAV	XFMR
4	N_7	RPL	TL
5	CAV	ESO	TL
6	FDI	AZL	TL
7	ANH	MFO	TL
8	AZL	SAA	TL
9	N_{10}	CAV	TL
10	ANH	ANH	XFMR

Table 6
$n-2$ contingency scenarios.

No.	Contingency 1			Contingency 2		
	From	To	Eq.	From	To	Eq.
1	XAV	BND	TL	CAV	CAV	XFMR
2	N_{11}	CAV	TL	SUR	N_4	TL
3	SUR	N_4	TL	AZL	SAA	TL
4	XAV	BND	TL	AZL	SAA	TL
5	MFO	XAV	TL	FDI	AZL	TL

For each contingency scenario, the first three components of the objective function were evaluated, i.e., transmission losses (f_1), voltage-related penalties (f_2), and current-related penalties (f_3). The fourth component, associated with multiple allocations at the same node, was not considered in this analysis, as the allocation configuration remained unchanged across all contingency cases. The results indicate an increase in all three evaluated objective function components under contingency conditions, as expected due to network topology degradation. However, these increases were not significant and did not lead to critical violations of operational limits. In the base case (i.e., the template) without allocating new data centers, the selected operating scenario already shows an average voltage of approximately 0.9 pu across all nodes. This behavior is expected, since the analysis is conducted under a high-loading operating condition.

For the first three-load set, the optimal allocation led to an increase in the number of nodes with voltage magnitudes below 0.9 pu under contingency conditions. On average, across the 15 contingency scenarios, voltages below this threshold were observed at six nodes, while in the most severe case, this number increased to 16 nodes. In this worst-case scenario, the average voltage magnitude of the affected nodes was approximately 0.86 pu, which remains close to the reference value observed in the base case. Regarding current constraints, overload-current limit violations were identified for the fourth $n-1$ contingency and for the second and fourth $n-2$ contingencies, with violations of 2.6%,

0.02%, and 0.17% above the maximum overload current, respectively. Given their small magnitudes, these violations are considered negligible.

For the second three-load set, a more pronounced voltage impact was observed. The average number of nodes with voltages below 0.9 pu increased to 8 across the contingency scenarios, while the worst-case contingency resulted in 28 nodes below this threshold. The lowest average voltage magnitude observed in this case was approximately 0.83 pu, which, although lower, remains reasonably close to the base-case average of 0.88 pu. No violations of the overload-current limits were observed for any of the $n-1$ or $n-2$ contingencies associated with this load set.

For the third three-load set, the contingency analysis resulted in an average of 5 nodes with voltage magnitudes below 0.9 pu and a maximum of 12 nodes in the worst-case scenario. In this most severe condition, the average voltage magnitude at the affected nodes was approximately 0.84 pu, again remaining close to the base-case reference value. Overload-current limit violations were identified for the fourth $n-1$ contingency and for the second and fourth $n-2$ contingencies, with violations of 7.7%, 0.002%, and 0.04%, respectively. The first value represents a more relevant, although still moderate, violation under worst-case conditions, whereas the remaining violations are negligible.

Finally, for the optimally allocated four-load set, the average number of nodes with voltages below 0.9 pu across the contingency scenarios was 5. The worst-case scenario resulted in 13 nodes below this threshold with an average voltage magnitude of approximately 0.88 pu, which is equal to the value observed in the base case without new data center allocations. An overload-current limit violation was observed only for the fourth $n-1$ contingency, with a current violation of approximately 2.9% above the maximum overload current, which is considered practically irrelevant.

Overall, the contingency analysis indicates that, although the optimal allocation of new data centers increases the number of nodes experiencing reduced voltage levels under abnormal operating conditions, the severity of these violations remains comparable to that observed in the base case. In addition, overload-current violations are either absent or limited, reinforcing the effectiveness of the proposed allocation methodology in enhancing the system's operational resilience under both $n-1$ and $n-2$ contingency scenarios. This behavior shows that the optimal allocation obtained through the proposed methodology may enhance the resilience of the transmission network when supplying large-scale, critical loads such as data centers.

5. Conclusion

This paper proposes an optimization-based methodology to support the integration of large-scale data centers into high-voltage transmission networks. The methodology combines a hosting capacity assessment with a PSO-based optimal allocation framework and a subsequent contingency analysis, all based on steady-state electrical calculations performed using ATP. By formulating a composite objective function that accounts for transmission losses, voltage constraints, current limits, practical substation allocation and line-tapping constraints, the proposed approach enables a physically meaningful and computationally feasible assessment of where and how new data centers can be connected within a predefined region of interest, without the need to build additional transmission infrastructure.

The results demonstrated that the proposed methodology is robust and effective across different data center loading scenarios. The hosting capacity assessment provided consistent estimates of the maximum admissible data center penetration. At the same time, the PSO-based optimization reliably converged to the global minimum when compared with brute-force enumeration, even as the problem dimensionality increased. The contingency analysis further showed that, although voltage reductions and current increases occur under abnormal operating conditions, their severity remains comparable to that of the base case, with overload-current violations either absent or limited. These results confirm the quality of the proposed allocation strategy and its ability to preserve acceptable operational margins under both normal and degraded network conditions.

The proposed methodology focuses on transmission-level hosting capacity and steady-state, contingency-based resilience. Dynamic behavior, transient stability, cascading outages, and detailed data center energy-management strategies are outside the scope of the study. More advanced technologies such as waste heat recovery, on-site generation, storage, and demand-side flexibility may reduce grid demand. However, these technologies do not affect the structure of the proposed methodology. Their effects can be represented through the net active and reactive power demand used as input data. Future work may incorporate these aspects, along with time-varying load profiles, weather-dependent ratings, and probabilistic contingency models.

From a practical perspective, the proposed methodology is directly applicable to real transmission networks and can support both planning and operational studies. In planning applications, it enables transmission operators to quantify hosting capacity, evaluate alternative allocation strategies, and identify potential reinforcement requirements in advance. From an operational perspective, the contingency-based assessment provides valuable insights into system resilience when supplying large, critical loads such as data centers. Owing to its modular structure and reliance on widely used simulation tools, the methodology can be readily adapted to various network topologies, operating scenarios, and regulatory frameworks, making it a flexible decision-support tool for integrating high-impact loads into modern power systems.

CRediT authorship contribution statement

Giovanni Manassero Jr.: Writing – original draft, Validation, Software, Methodology, Formal analysis, Data curation, Conceptualization. **Rodrigo Rozenblit Tiferes:** Writing – original draft, Validation, Software, Methodology, Formal analysis, Data curation, Conceptualization. **Thamiris Nascimento Ribeiro:** Writing – original draft, Visualization, Conceptualization. **Andrea Mazza:** Writing – original draft, Visualization, Conceptualization. **Enrico Pons:** Writing – original draft, Visualization, Conceptualization.

Declaration of competing interest

The authors declare that they have no known competing financial interests or personal relationships that could have appeared to influence the work reported in this paper.

Data availability

Data will be made available upon request.

References

[1] Abdelhady M, Iakovou E, Pistikopoulos EN. Optimal energy portfolio investment strategies for data centers under deep market uncertainty. Appl Energy 2026;410:127510.
[2] IEA. Energy and AI. Tech. Rep. International Energy Agency; Apr 2025.
[3] Liu W, et al. Online job scheduling scheme for low-carbon data center operation: an information and energy nexus perspective. Appl Energy 2023;338:120918.
[4] Ding Z, et al. Data center job scheduling and energy management under uncertain environments. IEEE Trans Ind Appl 2025;61(4):5489–500.
[5] Chen C, et al. Exploring the demand response potential of liquid-cooled data centers. Appl Energy 2026;412:127679.
[6] Bahrami S, Wong VWS, Huang J. Data center demand response in deregulated electricity markets. IEEE Trans Smart Grid 2019;10(3):2820–32.
[7] Zhang Y, et al. Unlocking the flexibilities of data centers for smart grid services: optimal dispatch and design of energy storage systems under progressive loading. Energy 2025;316:134511.
[8] Guo C, et al. Integrated planning of internet data centers and battery energy storage systems in smart grids. Appl Energy 2021;281:116093.
[9] Zhang Y, et al. Physics-guided deep reinforcement learning for optimized data center cooling and waste heat recovery utilizing aquifer thermal energy storage. Appl Energy 2026;402:126984.
[10] Yin X, et al. Exploiting internet data centers as energy prosumers in integrated electricity-heat system. IEEE Trans Smart Grid 2023;14(1):167–82.
[11] Cao Z, et al. Data center sustainability: revisits and outlooks. IEEE Trans Sustain Comput 2024;9(3):236–48.

[12] Huang H, et al. Power management optimization for data centers: a power supply perspective. IEEE Trans Sustain Comput 2025;10(4):784–803.
[13] Liang C, et al. Market-government dual-driven framework for reliability-centric planning of a computation-energy integrated system with data centers. Appl Energy 2025;396:126272.
[14] IEEE-PES. Data center growth and grid readiness. Tech. Rep. PES-TR 131 IEEE Power & Energy Society; May 2025.
[15] Liu T, et al. Carbon emission accounting during the construction of typical 500 kV power transmissions and substations using the carbon emission factor approach. Buildings 2024;14(1):145.
[16] Chen X, Ou Y. Carbon emission accounting for power transmission and transformation equipment: an extended life cycle approach. Energy Rep 2023;10:1369–78.
[17] Wang F, Lv C. A data center expansion scheme considering net-zero carbon operation: optimization of geographical location, on-site renewable utilization and green certificate purchase. Socio-Econ Plan Sci 2024;92:101789.
[18] Wang F, Lv C, Xu J. Carbon awareness oriented data center location and configuration: an integrated optimization method. Energy 2023;278:127744.
[19] Vafamehr A, et al. A framework for expansion planning of data centers in electricity and data networks under uncertainty. IEEE Trans Smart Grid 2019;10(1):305–16.
[20] Dong H, et al. A two-stage stochastic collaborative planning approach for data centers and distribution network incorporating demand response and multivariate uncertainties. J Clean Prod 2024;451:141482.
[21] Li W, et al. Distributionally robust chance-constrained planning for regional integrated electricity–heat systems with data centers considering wind power uncertainty. Appl Energy 2023;336:120787.
[22] Wu S, et al. Cyber-physical integrated planning of distribution networks considering spatial-temporal flexible resources. Prot Control Mod Power Syst 2024;9(3):142–56.
[23] Li B, et al. Joint network expansion planning with internet data center and charging stations for EV sharing system. IEEE Trans Ind Informat 2024;20(11):251–61.
[24] Ma B, et al. Multi-objective multi-stage distributionally robust chance-constrained low-carbon planning model for a novel integrated multi-energy microgrids incorporating data center considering real-time workload response and multiple uncertainties. Energy 2025;137110.
[25] Zhang Y, et al. A multi-objective interval optimization approach to expansion planning of active distribution system with distributed internet data centers and renewable energy resources. IET Gener Transm Distrib 2024;18(18):2999–3016.
[26] Su L, et al. Collaborative planning of distribution network, data centres and renewable energy in the power distribution IoT via interval optimization. Energies 2024;17(15):3623.
[27] Wang Z, et al. Distributionally robust planning for data center park considering operational economy and reliability. Energy 2024;290:130185.
[28] Lin J-H, Wu Y-K. Review of power system resilience concept, assessment, and enhancement measures. Appl Sci 2024;14(4):1428.
[29] Afzal S, et al. State-of-the-art review on power system resilience and assessment techniques. IET Gener Transm Distrib 2020;14(25):6107–21.
[30] Bhusal N, et al. Power system resilience: current practices, challenges, and future directions. IEEE Access 2020;8:064–086.
[31] Xiao Y, et al. A market for power system resilience provision. Appl Energy 2025;382:125335.
[32] Shami TM, et al. Particle swarm optimization: a comprehensive survey. IEEE Access 2022;10:031–061.
[33] Tiferes RR, Lima TRK, Manassero G. A methodology for investigating power transmission field-observed events based on digital twins combining physical and recorded data. IEEE Trans Ind Appl 2025;61(2):2813–24.